Ocean Acoustics: a novel laboratory for wave chaos

Steven Tomsovic
Department of Physics and Astronomy, Washington State University, Pullman, WA 99164-2814

Michael G. Brown
Rosenstiel School of Marine and Atmospheric Science, University of Miami, Miami, Florida 33149
(Dated: November 2, 2009)

One of the fascinating aspects of the field known colloquially as quantum chaos is the immense variety of physical contexts in which it appears. In the late 1980's it was recognized that ocean acoustics was one such context. It was discovered that the internal state of the ocean leads to multiple scattering of sound as it propagates and leads to an underlying ray dynamics which is predominantly unstable, i.e. chaotic. This development helped motivate a resurgence of interest in extending dynamical systems theory suitably for applying ray theory in its full form to a "chaotic" wave mechanical propagation problem. A number of theoretical tools are indispensable, including semiclassical methods, action-angle variables, canonical perturbation theory, ray stability analysis and Lyapunov exponents, mode approximations, and various statistical methods. In this tutorial, we focus on these tools and how they enter into an analysis of the propagating sound.

I. INTRODUCTION

Acoustic wave propagation through the ocean became a topic of immense physical interest in the latter half of the twentieth century. Beyond the evident sonar applications, acoustic waves offer a means with which to probe the ocean itself. It is possible to monitor bulk mean ocean temperatures over time, which gives important information for studying global warming, and to obtain other information about the internal state of the ocean, i.e. currents, eddies, internal waves, seafloor properties, etc. [1, 2]. However, this tutorial owes its existence rather to the recognition, beginning in the late 1980's, that the ray dynamics underlying propagation of acoustic waves is chaotic [3–6] and by inference, the subject can therefore be thought of as a unique problem in quantum chaos or perhaps better stated, wave chaos [7, 8]. Our focus here is on the interconnections and synergies arising between research in wave chaos and ocean acoustics. The interested reader is encouraged to consult reference works such as [1, 2] for more information about the motivations and foundations of ocean acoustics research.

Generally speaking, wave chaos studies require understanding theoretical techniques that can be loosely classified as random matrix [9, 10] and certain field theories [11, 12], and semiclassical theories of dynamical systems [13–15]. We have chosen to focus on those features and techniques that are most directly related to semiclassical and dynamical system theory approaches. For the research practitioner, it is critical to become conversant with eikonal expansions, saddle point integration techniques, WKB theory, mode approximations, action-angle variables, canonical perturbation theory, ray stability analysis, the geometry and measures of chaotic dynamics, amongst other skills. In order to simplify and focus the discussion, we cover these subjects as they apply to long range ocean acoustics under conditions in which acoustic interactions with the sea surface and seafloor can be neglected.

II. WAVES AND RAYS

The wave equation

$$\nabla^2\Phi(\vec{r},t) - \frac{1}{c^2(\vec{r},t)}\frac{\partial^2}{\partial t^2}\Phi(\vec{r},t) = 0 \tag{1}$$

accurately describes the acoustic waves of interest here, which are assumed to be sufficiently low frequency that dissipative losses can be neglected. The real part of $\Phi(\vec{r},t)$ is the acoustic pressure and $c(\vec{r},t)$ is the acoustic wave speed at location $\vec{r}$ and time t. At most midlatitude locations, the depth variations of $c(\vec{r},t)$ lie between approximately 1480 m/s and 1540 m/s. These variations are due mostly to the decrease in temperature with increasing depth and the nearly hydrostatic increase in pressure with depth; a 1° C increase leads to a 4 m/s increase in speed. Neglecting polar and coastal regions, the combined effects of temperatures and hydrostatic pressure lead to the formation of a sound speed minimum at approximately 1 km depth (in oceans that are typically approximately 5 km deep). The sound speed minimum is associated with a 'sound channel' [2] that causes sound to refract away from the sea surface and seafloor, thereby allowing sound to travel great distances with only small absorption- and scattering-induced energy losses.

FIG. 1: Measurements and simulations of acoustic intensity as a function of travel time and hydrophone depth in a long-range propagation experiment [18]. The top panel shows a single realization of the measured sound field. The middle panel shows a representative example of a parabolic equation simulation of the wavefield in a fairly realistic ocean environment that includes a simulated internal-wave-induced sound speed perturbation. The bottom panel shows a simulation of the wavefield in the same background environment but without the internal-wave-induced perturbation. In all three panels acoustic intensity relative to the peak intensity is color-coded in decibels. Taken with permission from Ref. [18].

Superimposed on the background sound speed structure are fluctuations with length scales from millimeters to thousands of kilometers and time scales from seconds to millennia. The low frequency sounds of interest for long-range propagation studies, with frequencies from tens to a few hundred Hz, are not sensitive to variability on scales shorter than approximately an acoustic wavelength [16]. It turns out that this roughly corresponds to the ocean's internal wave scale [17]; i.e. a scale associated with bulk water motions due to buoyancy forces. In the upper ocean, these motions have a lower length scale of approximately 10 m. Owing to these waves and other forms of ocean variability, the possibility that the resulting sound speed variations have the requisite symmetry for separating variables in the wave equation is entirely negligible. Furthermore, the variations are not weak enough to be ignored. As a consequence, exact solutions of realistic versions of Eq. (1) cannot be compactly expressed in terms of some known standard functions. In one set of representative experiments in the eastern North Pacific Ocean, propagation over a distance of approximately 3000 km was studied [18, 19]. Their Fig. 13, reproduced here in Fig. 1, illustrates the form of the acoustic signal received downrange and compares it to numerical simulations both with and without internal wave effects. A number of wavefield properties, including the vertical extension of the acoustic arrivals, intensity fluctuations, time biasing, signal coherence, arrival time spread, and arrival time wander, were measured and remain only partially understood [8].

Those physical processes that lead to the time dependence of $c(\vec{r},t)$ evolve on a much longer time scale than it takes for sound waves to pass through any given region. Internal waves, for example, are almost always treated as stochastic perturbations to the background. Midlatitude internal waves have a horizontal correlation distance of approximately 10 km and a correlation time of approximately 10 minutes in the upper ocean and much longer in the deep ocean. But it takes only about 6 seconds for sound to traverse 10 km. Locally therefore, $c(\vec{r},t)$ can be taken to be time-independent, "frozen" during the passage of sound waves. The assumption that the sound speed structure is a function of position only, $c = c(\vec{r})$, allows one to build up solutions to the full wave equation from a superposition of fixed-frequency solutions of a Helmholtz-like equation. Further, we shall assume that the scattering in the azimuthal direction is negligibly small, leading to cylindrical spreading (provided the range is not so large that earth's curvature must be taken into account) and $\vec{r} = (z, r)$, where z is depth in the ocean and r is range from the source. For a constant frequency source, i.e a pure sinusoidal source of angular frequency σ, the wave field has a frequency response, $\Phi_\sigma(z,r)$, where $\Phi(z,r,t) = \Phi_\sigma(z,r)\, e^{-i\sigma t}$. The Helmholtz-like equation in cylindrical coordinates is

$$\nabla^2\Phi_\sigma(z,r) + k^2(z,r)\Phi_\sigma(z,r) = 0 \ , \tag{2}$$

where the wave number $k(z,r) = \sigma/c(z,r)$.

A. The paraxial optical approximation

Two more approximations act together to further simplify the basic long-range ocean acoustics problem. The scattering and refraction that takes place is predominantly in the forward direction and at small angles. Steeply propagating wave energy is strongly attenuated by interactions with the bottom and not of interest. Taken together, a Fresnel approximation [20] is valid which gives the acoustic pressure as the product of an outgoing cylindrical wave and a slowly varying envelope function with a horizontal wavenumber $k_0 = \sigma/c_0$,

$$\Phi_\sigma(z,r) \ = \ \Psi_\sigma(z,r)\frac{e^{ik_0 r}}{\sqrt{r}} \tag{3}$$

whose governing equation is to an excellent approximation

$$\frac{i}{k_0}\frac{\partial}{\partial r}\Psi_\sigma(z,r) = -\frac{1}{2k_0^2}\frac{\partial^2}{\partial z^2}\Psi_\sigma(z,r) + V(z,r)\Psi_\sigma(z,r) \ . \tag{4}$$

The constant c_0 is a reference sound speed. There is some flexibility in the choice of the potential function $V(z,r)$. The most common choice is $V(z,r) = [1-(c_0/c(z,r))^2]/2$. An equally good choice of $V(z,r)$ is $(c(z,r)-c_0)/c_0$ (both

choices are first order accurate in $(c(z,r)-c_0)/c_0)$. In most underwater acoustic applications a good choice of c_0 is 1.5 km/s. The potential can be decomposed into two contributions, $V(z,r) = V_0(z) + V_1(z,r)$. The first term $V_0(z)$ describes the large scale wave guide effect mentioned earlier, which is either independent of range or very nearly so (adiabatic in the sense described below), and the second term $V_1(z,r)$ describes the remaining smaller scale variations due to all the physical processes at work in the ocean. Reference [1] contains details on all of the terms that have been dropped in arriving at Eq. (4) and has order of magnitude estimates for the size of the various dropped contributions.

Interestingly, this so-called parabolic equation, Eq. (4), maps without approximation onto the one-dimensional quantum mechanical Schrödinger equation through the substitutions $r \to t$ and $1/k_0 \to \hbar$. To the extent that the above stated approximations are valid, this equivalence shows that there exists a perfect analogy between wave chaos and quantum chaos. The measurable quantities and specific questions asked are different in the acoustic and quantum domains, as is the specific nature of the potential, but the fundamental structure of the two problems is common.

It should also be noted, however, that the acoustic wave chaos/quantum chaos analogy is limited to fixed frequency (monochromatic) acoustic wavefields. Equations (2-4) describe fixed frequency acoustic wavefields. The acoustic response to a transient source $s(t)$, whose Fourier transform is $\bar{s}(\sigma)$, can be expressed as a Fourier integral,

$$\Phi(z,r,t) = \frac{1}{2\pi}\int_{\infty}^{\infty} \bar{s}(\sigma)\Phi_\sigma(z,r)e^{-i\sigma t}d\sigma. \tag{5}$$

The quantity $\Phi(z,r,t)$ has no direct quantum mechanical counterpart.

B. Eikonal approximations

The terminology and techniques of semiclassical theories, ray theories, eikonal approximations, WKB theory, and saddle point integration are so profoundly intertwined that often they can be applied interchangeably. Depending on one's starting point, any of these approaches can be used to generate the connection between ray, transport, and wave equations. Generally speaking, in semiclassical theory an asymptotic approximation to the exact wave field is represented by a superposition of simpler waves, each one possessing a well defined phase with a slowly varying wavelength and envelope as a function of location. The resulting ray equations may have multiple solutions subject to the appropriate boundary conditions, and each one corresponds to one of the simpler waves and gives the phase. The transport equation describes the dynamical neighborhood of each ray and gives the slowly varying amplitude for the wave associated with that ray. A complete ray theory accounts for both the ray and transport equations. However, one often sees mention of ray theory in situations where it is clear that the authors are not considering the transport equations or even calculating the phases.

The theory can equally well be written down for non-stationary or stationary state/mode representations. Consider the non-stationary relations. Beginning with the eikonal ansatz

$$\Psi_\sigma(z,r) \approx \sum_j A_j(z,r)\exp\left(ik_0 S_j(z,r)\right) \ , \tag{6}$$

substitution into the parabolic equation and equating terms in like powers of k_0 generates the Hamilton-Jacobi and transport equations of classical mechanics [21], respectively,

$$\begin{aligned} 0 &= \frac{\partial}{\partial r}S(z,r) + \frac{1}{2}\left[\frac{\partial}{\partial z}S(z,r)\right]^2 + V(z,r), \\ 0 &= \frac{\partial}{\partial r}A^2(z,r) + \frac{\partial}{\partial z}\left[A^2(z,r)\frac{\partial}{\partial z}S(z,r)\right] \ . \end{aligned} \tag{7}$$

The solution to the Hamilton-Jacobi equation for $S(z,r)$, which is referred to as Hamilton's principal function, can be constructed by integrating the equation

$$\frac{\mathrm{d}}{\mathrm{d}r}S(z,r) = p\frac{\mathrm{d}z}{\mathrm{d}r} - \mathcal{H}(p,z;r) \tag{8}$$

together with the ray equations (Hamilton's equations)

$$\frac{dz}{dr} = \frac{\partial\mathcal{H}(p,z;r)}{\partial p}, \quad \frac{dp}{dr} = -\frac{\partial\mathcal{H}(p,z;r)}{\partial z} \tag{9}$$

where

$$\mathcal{H}(p,z;r) = \frac{p^2}{2} + V(z,r) \tag{10}$$

is the Hamiltonian. Discrete values $A_j(z,r)$ and $S_j(z,r)$ of $A(z,r)$ and $S(z,r)$ appear in Eq. (6). These discrete variables correspond to those rays, often referred to as 'eigenrays', that connect fixed source and receiver locations. The eikonal function $S(z,r)$ in Eq. (6) is a reduced travel time $S(z,r) = c_0\mathcal{T}(z,r) - r$ where $\mathcal{T}$ is ray travel time. Returning briefly to the analogy between quantum chaos and wave chaos, note that it follows from the relationship $S(z,r) = c_0\mathcal{T} - r$ that in the ocean acoustic context, the travel time is a measurable physical manifestation of Hamilton's principal function for a trajectory. In a quantum mechanical context, there is the association of $S(z,r)$ with a phase only.

The transport equation can be solved assuming a point source. For the j-th eigenray

$$A_j(z,r) = A_{0j}\,|q_{21}|_j^{-1/2}\,e^{-i\mu_j\frac{\pi}{2}}. \tag{11}$$

The matrix element q_{21}, defined below, describes the spreading of a ray bundle in the infinitesimal neighborhood of the j^{th} ray. At any fixed r, one has

$$\begin{pmatrix} \delta p \\ \delta z \end{pmatrix} = Q_r(p_0,z_0)\begin{pmatrix} \delta p_0 \\ \delta z_0 \end{pmatrix}\ , \tag{12}$$

where the stability matrix [22]

$$Q_r(p_0,z_0) = \begin{pmatrix} q_{11} & q_{12} \\ q_{21} & q_{22} \end{pmatrix} = \begin{pmatrix} \left.\frac{\partial p}{\partial p_0}\right|_{z_0} & \left.\frac{\partial p}{\partial z_0}\right|_{p_0} \\ \left.\frac{\partial z}{\partial p_0}\right|_{z_0} & \left.\frac{\partial z}{\partial z_0}\right|_{p_0} \end{pmatrix}\ . \tag{13}$$

We usually drop the initial condition arguments for brevity, but clearly each initial condition leads to a unique range dependent stability matrix. Elements of this matrix evolve according to

$$\frac{d}{dr}Q_r = K_r Q_r \tag{14}$$

where $Q_{r=0}$ is the identity matrix, and

$$K_r = \begin{pmatrix} -\frac{\partial^2\mathcal{H}}{\partial z\partial p} & -\frac{\partial^2\mathcal{H}}{\partial z^2} \\ \frac{\partial^2\mathcal{H}}{\partial p^2} & \frac{\partial^2\mathcal{H}}{\partial z\partial p} \end{pmatrix}. \tag{15}$$

At caustics q_{21} vanishes and the Maslov index μ advances by one unit. Jumps in the phase index actually preserve smooth phase variation for problems with initial wave packets. At these points diffractive corrections to Eq. (11) must be applied. The normalization factor A_{0j} is chosen in such a way that close to the source it matches the Green function for the parabolic equation.

III. THE SEPARABLE PROBLEM – RAYS AND MODES

In this section we focus on the special case in which the sound speed is a function of depth only, $c(z,r) = c(z)$ and $V(z,r) = V_0(z)$. For this special class of problems the parabolic wave equation admits separable solutions $\Psi_\sigma(z,r) = Z(z;\sigma)R(r;\sigma)$. One such solution, involving an expansion in normal modes, is discussed below. Solving the ray equations, Eq. (9), is also greatly simplified in this case. A particularly useful technique to accomplish this goal is to make use of action-angle variables (I,θ); these variables are introduced in the next subsection. To make our discussion concrete, we focus on the most common class of deep ocean acoustic waveguides in which $c(z)$ has a single minimum. For this class of problems there exists rays and modes with two internal turning depths that interact negligibly with the surface and the bottom.

As noted earlier, the class of problems treated here is too idealized to constitute a solution to Eq. (4) under realistic conditions. Rather, the reason for discussing this problem is that almost all of the material introduced here turns out to be very useful as the basis of perturbation expansions that apply when a range-dependent environmental perturbation is introduced, as described in the sections that follow. In addition to this caveat, note that we do not consider here situations where tunnelling and diffraction are of paramount interest. Caustic and turning point corrections, which can be accounted for by uniform approximations, are also not discussed here, as those subjects are beyond the scope of this tutorial and not the primary issue.

A. Rays and action-angle variables

Action-angle variables are introduced by a canonical transformation from (p, z) to (I, θ) [21]. The same transformation replaces $\mathcal{H}(p, z)$ by $\mathcal{H}(I)$; in fact, $\mathcal{H}(p, z) = \mathcal{H}(I)$. The numerical values of $\mathcal{H}$ are unchanged by the canonical transformation, but the dependence of $\mathcal{H}$ on the independent variables is of course different in $\mathcal{H}(p, z)$ and $\mathcal{H}(I)$.) Note also that if $c(z, r) = c(z)$, $\mathcal{H}$ is constant following rays. For the two internal turning point class of problems the action is defined by

$$I = \frac{1}{2\pi} \oint p dz = \frac{1}{\pi} \int_{\check{z}(\mathcal{H})}^{\hat{z}(\mathcal{H})} dz \sqrt{2[\mathcal{H} - V_0(z)]} \tag{16}$$

where $V_0(\hat{z}(\mathcal{H})) = V_0(\check{z}(\mathcal{H})) = \mathcal{H}$. The transformation from (p, z) to (I, θ) makes use of the generating function

$$G(I, z) = \begin{cases} \int_{\check{z}(\mathcal{H})}^{z} dz' \sqrt{2[\mathcal{H} - V_0(z')]}, & p > 0 \\ \pi I + \int_{z}^{\hat{z}(\mathcal{H})} dz' \sqrt{2[\mathcal{H} - V_0(z')]}, & p < 0. \end{cases} \tag{17}$$

where $p = \partial G/\partial z$ and $\theta = \partial G/\partial I$. As z varies from one turning point to the next and back, $\check{z} \to \hat{z} \to \check{z}$, θ varies from $0 \to \pi \to 2\pi$ and for each complete ray cycle θ increases by 2π. The action-angle form of the ray equations are

$$\frac{dI}{dr} = -\frac{\partial \mathcal{H}}{\partial \theta} = 0, \qquad \frac{d\theta}{dr} = \frac{\partial \mathcal{H}}{\partial I} = \omega(I) \tag{18}$$

whose solution is $I(r) = I_0$, $\theta(r) = \theta_0 + \omega(I)r$. In this case, the total derivative of the Hamiltonian with respect to I is identical to the partial derivative and gives the angular frequency of motion. Similarly, and consistently, the transformed stability equations and solutions are

$$Q_r(I_0, \theta_0) = \begin{pmatrix} \frac{\partial I}{\partial I_0}\Big|_{\theta_0} & \frac{\partial I}{\partial \theta_0}\Big|_{I_0} \\ \frac{\partial \theta}{\partial I_0}\Big|_{\theta_0} & \frac{\partial \theta}{\partial \theta_0}\Big|_{I_0} \end{pmatrix} = \begin{pmatrix} 1 & 0 \\ \omega'(I_0)r & 1 \end{pmatrix}, \tag{19}$$

where the quantity $\omega'(I) = d\omega(I)/dI$ describes the rate of shearing in the dynamics, i.e. how much the angular frequency of the motion shifts with a change in I.

The reduced travel time S (Hamilton's principal function) evolves according to

$$\frac{dS}{dr} = I\omega(I) - \mathcal{H}(I) + \frac{d}{dr}(G - I\theta) \tag{20}$$

which can also be integrated by inspection. The generating function G increases monotonically from 0 at $z = \check{z}$ to πI at $z = \hat{z}$ to $2\pi I$ at $z = \check{z}$. Because θ increases by 2π during each ray cycle, the endpoint correction term $G - I\theta$ in Eq. (20) oscillates about zero. Except at short range, for most purposes this term gives a negligibly small contribution to S. In addition, since $I(r) = I_0$, i.e. the action is a constant, it is possible to consider the depth z as depending on the angle variable $z_{I_0}(\theta)$, oscillating up-down one full cycle for θ increasing by 2π. The angular frequency $\omega(I) = 2\pi/R_\ell(I)$ where $R_\ell(I)$ is the spatial 'period' in r of a ray. (The subscript ℓ denotes loop.)

Systems of the type just described are referred to as integrable and their phase space ($\{p, z\}$) is filled (often said to be foliated) by a continuous family of manifolds, i.e. continuous sets of phase space points called tori. In the class of systems discussed above having a single degree of freedom, every ray is periodic and forms its own torus. In higher degrees of freedom, each ray lies on a particular torus, and if it is not periodic, then it will come arbitrarily close to every point on the torus eventually. If a ray is periodic, then a continuous family of like periodic rays combine to form the torus.

In anticipation of the material presented in Sect. IV.B, whose focus is wavefield properties in the presence of scattering by small-scale inhomogeneities, some brief remarks about wavefield structure in the absence of such scattering are in order. A typical experimental arrangement involves the production of a transient signal by a compact source at a fixed submerged location. The resulting transient wavefield is measured at a horizontal distance (range) r, typically with concurrent measurements at many depths. The challenge is to explain the distribution of acoustic energy in (z, t) as a function of range and central frequency.

From the action-angle description, a canonical transformation is needed to obtain the depth dependence of the wavefield (which follows the depth dependence of the rays); little more can be generally stated about this dependence. If one focusses on the temporal distribution of energy, without regard to the corresponding ray depth, a very simple picture emerges. This temporal dependence is described by the action-angle form of the ray equations, and proves to

be controlled by the quantity $\omega'(I)$. First, note that it follows from Eqs. (11,19), that geometric intensities (squared amplitudes) are proportional to the ray spreading factor $1/|q_{21}| \propto 1/|\omega'(I)r|$. Next, recall that the ray travel time $T = (S + r)/c_0$. It follows from this expression and Eq. (20) that at fixed r, $dT/dI = \omega'(I)r/c_0$. Because I is a ray label this simple equation shows that the dispersion or temporal spreading of the wavefield in the ray limit is controlled entirely by $\omega'(I)$. The foregoing comments reveal that when $c(z, r) = c(z)$ geometric amplitudes are controlled to a good approximation by $\omega'(I)$ and that, without approximation, geometric travel time dispersion is controlled by $\omega'(I)$.

B. Modes and action quantization

[41]

For a point source at $(z, r) = (z_s, 0)$, the modal expansion of the solution to the parabolic wave equation, Eq. (4), has the form

$$\Psi_\sigma(z, r) = \sum_m \varphi_m(z_s; \sigma)\varphi_m(z; \sigma)e^{ik_m r} \qquad r \geq 0 \tag{21}$$

where the eigenfunctions $\varphi_m(z)$ and eigenvalues $k_m = k_0\mathcal{H}_m$ satisfy

$$\frac{1}{2}\frac{d^2\varphi_m}{dz^2} + k_0^2(\mathcal{H}_m - V_0(z))\varphi_m = 0. \tag{22}$$

Together with appropriate boundary conditions, Eq. (22), defines a Sturm-Liouville problem, guaranteeing that the functions $\varphi_m(z; \sigma)$ are complete and orthogonal,

$$\int dz\ \varphi_m(z; \sigma)\varphi_n(z; \sigma) = \delta_{m,n}. \tag{23}$$

In the semiclassical (WKB) approximation, each mode can be expressed as a superposition of an up- and down-going waves with reflection coefficients $e^{i\phi_u}$, $e^{i\phi_l}$ at the upper and lower turning depths respectively. If these reflections take place without loss of energy then ϕ_u and ϕ_l are real. Also, in the WKB approximation $\mathcal{H}_m = \mathcal{H}(I_m)$ and

$$k_0 I_m = m - \frac{\phi_u + \phi_l}{2\pi}, \qquad m = 0, 1, 2, \ldots \tag{24}$$

For modes with internal turning depths $\phi_u = \phi_l = -\pi/2$ and the quantization condition (24) reduces to

$$k_0 I_m = m + \frac{1}{2}. \tag{25}$$

The quantization condition, Eq. (24) or Eq. (25), is seen to be a statement that the action I is quantized. This relationship provides a simple and direct connection between the ray description and the asymptotic mode description of the underwater sound field.

IV. THE NONSEPARABLE PROBLEM

The results presented so far apply to the idealized separable problem, $c(z, r) = c(z)$. The utility of those results stems in large part from the observation that those results provide a basis for two important classes of nonseparable problems. First is the adiabatic problem in which the range-dependence is assumed to be slow $c(z, r) \to c(z, \varepsilon r)$. One can extend the action-angle formalism and modal expansion to incorporate this very slow range dependence into the definition of the action-angle variables themselves. This class of problems is fairly well understood (see, e.g. [23]) and will not be discussed further except to note that the principal results are that the action I is an adiabatic invariant, $dI/dr = O(\varepsilon^2)$ [compare to the first relation of Eq. (18)] and mode coupling is negligible in a lower frequency regime. The latter statement follows heuristically from Eq. (24 or 25) and the smallness of dI/dr. The second class of nonseparable problems for which the action-angle description has proven to be very useful is the class for which $c(z, r) = c(z) + \varepsilon\delta c(z, r)$. This class of problems is critical to understanding ocean acoustics and gives rise to wave chaos in that context.

A. Stability analysis in range-dependent systems: numerical approach

In principle, it is by way of the stability analysis, all of whose information is embedded in Q_r, that one assesses how regular (stable) or chaotic (unstable) the ray dynamics are. A certain amount of analytical mathematics has been developed in this domain, which can be loosely termed KAM theory [24] after Kolmogorov, Arnold, and Moser, which is discussed in the next subsection. Before entering that discussion however, consider that Eqs. (12-14) are quite suitable for numerical investigations since they present the same level of difficulty as Hamilton's equations for determining the rays themselves. In fact, the same numerical techniques are invoked for both.

From a numerical analysis perspective, an important property of chaotic rays is that they exhibit extreme sensitivity to initial conditions in their local neighborhood, which expresses itself as an exponential growth in the separation of nearby rays. For finite range r, the growth can be approximately characterized by a positive, finite-range, stability exponent, ν_r [25],

$$\nu_r = \frac{\ln |\mathrm{Tr}(Q_r)|}{r} \ . \tag{26}$$

In contrast to the Lyapunov exponent, which can roughly be thought of as the infinite-range limit

$$\nu_L = \lim_{r\to\infty} \nu_r \ , \tag{27}$$

ν_r depends on the particular ray, varies with range, and thus fluctuates. It turns out that Eq. (26) is not sophisticated enough to answer questions of instability in a range-dependent environment. What follows illustrates the main difficulty and resolution.

Although regular rays do not separate exponentially, they can exhibit algebraic range dependence [26], and this leads to some ambiguity as to whether a ray is actually regular or chaotic (stable or unstable). For example, consider a one-degree-of-freedom system for which $\mathcal{H}(p, z; r)$ is periodic in range. If at range r a ray corresponds to a periodic orbit (i.e. $z_0 = z_r$ and $p_0 = p_r$), then the trace of its stability matrix indicates [27]

$$|\mathrm{Tr}Q_r| = \begin{cases} < 2 & \text{orbit is stable and local dynamics is rotational (regular)} \\ = 2 & \text{orbit is marginally stable and local dynamics is shearing (regular)} \\ > 2 & \text{orbit is unstable and local dynamics is hyperbolic (chaotic)} \end{cases} \tag{28}$$

and there is no ambiguity. It turns out that for such systems there is a simpler approach to getting at this information, the construction of Poincaré surfaces of section. By considering a section of the available phase space that the rays pass through, recording where rays intersect the section, gives an image of the stability throughout the phase space. This is because the recorded points of a stable or marginally stable ray must lie on a lower dimensional set than a chaotic ray. The advantage is that without calculating Q_r one can see at a glance in low-dimensional systems which parts of the phase space contain regular rays and which parts contain chaotic rays. For non-periodic dynamical systems, this construction of a Poincaré surface of section does not work. How can we still get at least an approximate sense for which parts of phase space are regular and which parts are chaotic?

There is no shortcut, one must consider Eqs. (12,14). It is worth showing a concrete example. A simple periodic map is given by the standard map [28],

$$\begin{aligned} p_{j+1} &= p_j - \frac{K}{2\pi}\sin 2\pi z_j \qquad \mod 1 \\ z_{j+1} &= z_j + p_{j+1} \qquad \mod 1 \end{aligned} \tag{29}$$

For certain values of K, the phase space contains both regular and chaotic rays. See the upper left panel of Fig. (2). Each solid line indicates a single ray possessing regular motion whereas the randomly-looking filled in zones indicate the region of phase space belonging to chaotic rays.

The above relations in Eq. (28) for $|\mathrm{Tr}(Q_r)|$ are not true even for other-than-full-period periodic orbits, and certainly not true for non-periodic orbits or range-dependent dynamical systems. In other words, if one applies Eq. (28) to a large ensemble of rays with initial conditions uniformly covering the available phase space, one would construct something like a surface of section that has the appearance of the upper right panel in Fig. (2). It possesses some similarities to the proper surface of section, but is obviously incorrect since the vast majority of stable orbits mistakenly show up as unstable.

There is, nevertheless, a means by which to separate approximately stable and unstable regions of phase space as a function of propagation range; i.e. the proportion of rays mimicking stable behavior up to some range will decrease with increasing range of propagation. It is easy to recognize the origin of the difficulty with a trivial example. Imagine

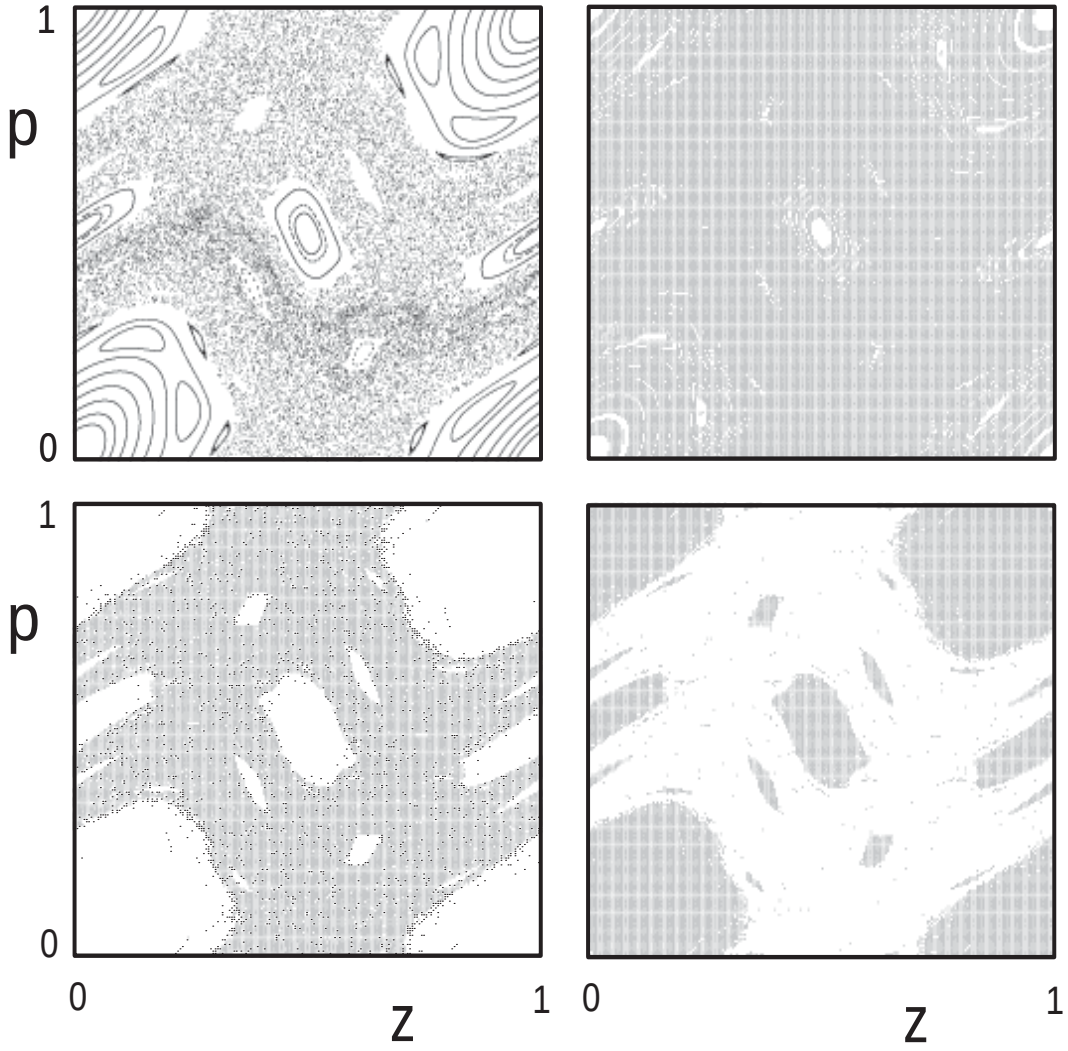

FIG. 2: An approximate surface of section. The upper left panel shows the true surface of section for the standard map for a value of $K = 1.365$ found by running a small number of rays for thousands of iterations of the map. The points falling on lines are in regular regions and the seemingly-randomly-placed points fill the chaotic zone. The upper right panel shows those initial conditions taken from a large uniform ensemble for which $|\mathrm{Tr}Q_r| > 2$ after 100 iterations of the map. By comparison to the upper left panel, it demonstrates that the majority of the stable orbits are mistakenly determined to be unstable if one blindly follows the criterion of Eq. (28) for non-periodic orbits. The bottom left panel shows the initial conditions for which a fit as described in the text gives a positive finite-range Lyapunov exponent. The lower left panel shows those initial conditions for which the same fit gives a vanishing Lyapunov exponent to within the precision allowed (determined by the range of propagation considered). By comparing to the information contained in the upper left panel, it demonstrates that this method approximately separates correctly, the unstable and stable rays, respectively.

an orbit exists which is periodic after two iterations of its map, and that its stability matrix for a single period is given by $Q = Q_2 Q_1$. In this example, suppose

$$Q_2 = \begin{pmatrix} 1 & -1 \\ \frac{3}{2} & -\frac{1}{2} \end{pmatrix} \qquad Q_1 = \begin{pmatrix} \frac{1}{2} & 1 \\ -\frac{1}{2} & 1 \end{pmatrix} \tag{30}$$

For a full period and n retracings, the orbit would be seen to be marginally stable;

$$Q = \begin{pmatrix} 1 & 0 \\ 1 & 1 \end{pmatrix} \qquad \text{and} \qquad Q^n = \begin{pmatrix} 1 & 0 \\ n & 1 \end{pmatrix} \tag{31}$$

However at odd integer iterations,

$$Q_1 Q^n = \begin{pmatrix} \frac{1}{2}+n & 1 \\ -\frac{1}{2}+n & 1 \end{pmatrix} \tag{32}$$

giving $\mathrm{Tr}(Q_1 Q^n) = \frac{3}{2} + n$, which grows without bound as n increases. It is incorrect to identify chaotic non-periodic rays with $|\mathrm{Tr}(Q_r)| > 2$ and regular ones with $|\mathrm{Tr}(Q_r)| \leq 2$.

Rather it is necessary to distinguish between exponential growth and algebraic growth (often found with oscillatory behavior as above). Using the relation (not valid for ranges that are very short) [26]

$$|Tr(Q_r)| \sim r^{\mu} \mathrm{e}^{\alpha+\nu r} \tag{33}$$

a least squares method can be generated to determine whether exponential growth is occuring. Minimizing the function

$$F(r) = \int_{r_{min}}^{r} \mathrm{d}s \left(\ln|\mathrm{Tr}(Q_s)| - \alpha - \mu \ln s - \nu s\right)^2 \tag{34}$$

with respect to $\{\alpha, \mu, \nu\}$ leads to an inhomogeneous set of three linear equations that can be solved using a standard method involving a ratio of determinants; only the solution for ν is of interest. The coarse graining is evident here. Roughly speaking, if up to the maximum propagation range, $\nu r \lesssim 1$ or 2, it is not possible to distinguish algebraic growth from exponential. Thus, as a practial matter, we consider rays for which $\nu \leq 2/r$ as regular. The bottom two panels of Fig. (2) show the improvement that results from incorporating the least squares analysis. The separation of regular and chaotic trajectories now approximates the true dynamics as seen in the Poincaré surface of section. This approach does not depend upon whether a system is non-periodic or not.

B. Chaos: resonances, KAM theory, and extreme sensitivity

Turning now to analytic mathematical theory associated with the problem for which $c = c(z) + \delta c(z, r)$, we shall assume that the perturbation term δc is an order ϵ multiperiodic function of N spatial frequencies $\Omega_i, 1 = 1, 2, \ldots N$,

$$\delta c = \delta c(z, \Omega_1 r, \Omega_2 r, \ldots, \Omega_N r). \tag{35}$$

The only restriction on N is that it is finite. This class of perturbations is sufficiently large that it encompasses commonly used models of ocean sound speed perturbations – due, for example, to internal waves [29].

Consistent with Eq. (35), the action-angle form of the Hamiltonian is

$$\mathcal{H}(I, \theta, r) = \mathcal{H}_0(I) + \varepsilon \mathcal{H}_1(I, \theta, \Omega_1 r, \Omega_2 r, \ldots, \Omega_N r). \tag{36}$$

and the corresponding ray equations are

$$\frac{dI}{dr} = -\varepsilon \frac{\partial \mathcal{H}_1}{\partial \theta}, \qquad \frac{d\theta}{dr} = \omega(I) + \varepsilon \frac{\partial \mathcal{H}_1}{\partial I}. \tag{37}$$

Here the action-angle variables are defined in the background environment, i.e. Eqs. (16,17) apply except $\mathcal{H}$ is replaced by $\mathcal{H}_0$. Also, consistent with the approximations made above, $\varepsilon \mathcal{H}_1 = \delta c / c_0$. Similarly, Eqs. (12-14) have an action-angle form by the substitution $(p \to I, z \to \theta)$.

The stability of trajectories in a Hamiltonian system under a small perturbation to an integrable system is addressed by the previously mentioned KAM theory [24]. The principal result is the KAM theorem, of which there are many variants. According to each such variant of the theorem most of the tori of the unperturbed system, on which trajectories lie, survive under a sufficiently small perturbation provided certain conditions are met. Proofs of KAM theorems for systems of the form of Eqs. (36,37) can be found in [30, 31]. Both of these references assume that $\mathcal{H}_1$ is a quasiperiodic function of the timelike variable, r. With no loss of generality, commensurable (rationally related) frequencies Ω_i in Eq. (36) may be eliminated, reducing that system to a quasiperiodic system.

In realistic ocean environments one generally does not encounter situations in which the perturbation is so small that unperturbed tori survive in the perturbed environment. One might then question why KAM theory should be emphasized. The relevance of KAM theory to systems of this type stems in large part from the insight that KAM theory provides into the mechanism that leads to torus destruction. That mechanism is the excitation and overlapping of resonances when the unperturbed frequency of motion $\omega(I)$ is rationally related to the vector of forcing frequencies $\mathbf{\Omega}$; the resonance condition is $k\omega(I) = \mathbf{j} \cdot \mathbf{\Omega}$ where k is an integer and $\mathbf{j}$ is a vector of integers. Low-order resonances,

for which both k and all of the elements of $\mathbf{j}$ are small are most strongly excited. Each resonance has a characteristic width (in I or ω), which scales like

$$\Delta I \propto \sqrt{\varepsilon/|\omega'(I)|}, \qquad \Delta\omega \propto \sqrt{\varepsilon|\omega'(I)|} \tag{38}$$

where $\omega'(I)$ is evaluated on the resonant torus; note that the resonance width also falls off rapidly with increasing k in a characteristic way. Refinements to the estimates Eq. (38) on degenerate tori where $\omega'(I) = 0$ are presented in [32]. When resonances overlap intervening tori are broken; this leads to Chirikov's definition of chaos [33].

A second point to emphasize is that among the class of systems of the form Eq. (36), the choice $N = 1$ is special only insofar as it allows the construction of Poincare sections (as discussed in the previous subsection) – by viewing trajectories stroboscopically at r-values that are integer multiples of the period of the perturbation $2\pi/\Omega_1$, modulo an arbitrary constant. While this is an important simple visualization tool for the $N = 1$ special case, it should be emphasized that, independent of N: 1) KAM theory holds; 2) torus destruction is caused by the excitation and overlapping of resonances whose widths scale like Eq. (38); and 3) surviving tori or secondary islands that are formed when tori are broken serve as impenetrable barriers to other trajectories (for an explanation of why this is so, see [32]). Taken together, these properties reveal that the essential physics of torus destruction and ray chaos are independent of N. Also, the foregoing comments strongly suggest that the most important environmental property controlling the physics of torus destruction and ray chaos is $\omega'(I)$, a property of the unperturbed environment. We will return to this point below. It is worth connecting heuristically the preeminent role of $\omega'(I)$ with Eq. (14). The matrix K_r constructed along a ray determines Q_r and ultimately everything about a ray's stability. From the action-angle form of Eq. (15) and the action-angle form of Hamilton's Eqs. (37), only the lower left element of K_r has a contribution which is not of $O(\varepsilon)$; its leading behavior is given by $\omega'(I) = \mathrm{d}^2\mathcal{H}_0/\mathrm{d}I^2$ (see Eq. 19).

While the essential physics of ray chaos is independent of N, it should be noted that for small N (and for $N = 1$, in particular) torus destruction is dominated by the excitation of a small number of low order resonances; for small ε most of the tori that are not entrained into one of the low-order resonances survive under perturbation. In contrast, when N is large and a broad range of Ω_i's are present, many low order resonances are excited and, typically, all of the original tori are destroyed. Numerical evidence strongly suggests that this is the case in typical deep ocean underwater acoustic environments, where for internal-wave-induced sound speed perturbations $\varepsilon = O(\delta c/c_0) = O(10^{-3})$. Under such conditions it is natural to adopt a stochastic framework to describe ray motion and underwater acoustic wavefields approximately.

C. Stochastic approximations: action diffusion

In the presence of a weak but highly structured sound speed perturbation field, N large in Eq. (35), a very useful model of sound scattering involves the diffusion of rays in action I, which implies spreading of acoustic energy. Conceptually, this model follows from the assumption that at each of a sequence of discrete scattering events, rays are scattered from one action surface to another. It is easiest to illustrate the basic assumptions and the utility of the model by discussing an example.

Consider the scattering-induced perturbation to the range of a ray, Δr, as a result of undergoing a sequence of n scattering events. In typical deep ocean environments steep rays are most strongly scattered near their upper turning depths, leading to the so-called apex approximation in which all scattering takes place at these locations. After n such scattering events

$$\Delta r_n = \frac{dR_\ell(I_0)}{dI} \sum_{i=1}^{n} (I_i - I_0) \tag{39}$$

where $R_\ell(I)$ is a ray cycle (or loop) distance, partial ray loops have been neglected, I_0 is the unperturbed ray action, and I_i is the action after the ith scattering event. Let δI_j denote the jump in I at the jth scattering event. Then

$$I_i - I_0 = \sum_{j=1}^{i} \delta I_j. \tag{40}$$

To a good approximation scattering events can be assumed to be independent and δI_j can be assumed to be a delta-correlated zero-mean random variable,

$$\langle \delta I_j \rangle = 0, \qquad \langle \delta I_j \delta I_k \rangle = \langle (\delta I)^2 \rangle \delta_{jk}. \tag{41}$$

where $\langle \ldots \rangle$ denotes ensemble averaging. It follows from Eqs. (39-41) that $\langle (\Delta I_n)^2 \rangle = \langle (I_n - I_0)^2 \rangle = \langle (\delta I)^2 \rangle n \simeq \langle (\delta I)^2 \rangle r / R_\ell$, and that for large n

$$\langle (\Delta r)^2 \rangle = \left(\frac{dR_\ell(I_0)}{dI} \right)^2 \langle (\delta I)^2 \rangle \frac{1}{3} \left(\frac{r}{R_\ell} \right)^3 . \tag{42}$$

But $\omega(I) = 2\pi / R_\ell(I)$ so $\omega'(I) = -2\pi R'_\ell(I) / (R_\ell(I))^2$. We may replace $\langle (\delta I)^2 \rangle / R_\ell$ by a general action diffusivity D where $\langle (I(r) - I_0)^2 \rangle = Dr$. With these substitutions

$$\langle (\Delta r)^2 \rangle = \left(\frac{\omega'(I_0)}{\omega(I_0)} \right)^2 D \frac{r^3}{3}. \tag{43}$$

In spite of the seemingly strong assumptions on which Eq. (43) is based, this expression turns out to provide a very good approximation to distributions of range spreads of rays in realistic deep ocean environments. Two features of this expression are noteworthy. First, the scattering process is completely parameterized by the action diffusivity D (which is typically a slowly-varying function of I_0). Second, the observable $(\Delta r)_{rms}$ is proportional to $\omega'(I_0)$. In other words, the scattering is parameterized entirely by D, but the scattering is amplified by an amount proportional to $\omega'(I_0)$ in the observable $(\Delta r)_{rms}$.

The argument just presented focused on a ray-based calculation. It should be emphasized, however, that the central ingredient of the scattering argument presented – the diffusion of action – is equally relevant to the modal description of the sound field. The reason is that it follows from the quantization condition (25) that scattering of mode energy from mode m to $m \pm 1$ is accompanied by a jump in action by the amount $1/\sigma$. Thus as energy diffuses in action it also diffuses in mode number, $(\Delta m(r))_{rms} = \sigma \sqrt{Dr}$. This simple approximation provides a direct connection between ray- and mode-based descriptions of wavefields in the presence of weak scattering.

With the above as background we are now in a position to state, without derivation, the dependence of various wavefield properties on $\omega'(I)$ and the action diffusivity D. Most of the properties enumerated here are measurable. All of the derivations are straightforward (most are very simple), but are not presented here. Several different measures of time spreads that are constrained in different ways, corresponding to different experimental scenarios, have been shown to be proportional to $\omega'(I)$ [34, 35]. Both the spatial and temporal spreading of directionally narrow beams have been shown to proportional to $|\omega'(I)|D$ [36]. The diffractive contribution to the effective width of a ray (the Fresnel zone width) has been shown to be approximately proportional to $\sqrt{|\omega'(I)|}$ [37]. The scattering-induced contribution to the effective width of a ray has been shown to be proportional to $|\omega'(I)|D$ [37]. In a transient wavefield, a modal group arrival can be defined as the contribution to the wavefield associated with a fixed mode number, but containing frequencies across the entire excited frequency band. The deterministic dispersive contribution to the modal group time spread has been shown to be proportional to $|\omega'(I)|$ [38], and the scattering-induced (associated with mode coupling) contribution to the modal group time spread has been shown to be proportional to $|\omega'(I)|D$ [38]. Also, numerical simulations reveal that average Lyapunov exponents scale like $|\omega'(I)|$ [34].

The scattered wavefield properties just described have two common properties. First, the scattering process itself is described by the diffusion of rays (and hence also acoustic energy) in I. This diffusion process is parameterized by the diffusivity D. Second, observable wavefield properties are proportional to $\omega'(I)D$. In other words, the scattering itself, as embodied in D, is amplified by a factor that is proportional to $\omega'(I)$. Thus, a large scattering-induced time spread, for instance, could be the result of a large $\omega'(I)$ together with a modest value of D. The important role of $\omega'(I)$ in controlling observable scattering-induced wavefield properties (e.g., time spreads) is not well appreciated by underwater acousticians. Rather, it is widely assumed, incorrectly, by most practitioners in the field that scattering-induced contributions to wavefield properties are controlled entirely by the sound speed perturbation field $\delta c(z, r)$. Finally, we note that the simple arguments above leading to Eq. (43) have been put on a more rigorous basis by making use of results from the study of stochastic differential equations [39]. As above, the critical conceptual notion is diffusion of rays in I. Part of the utility of that approach is that it leads to explicit ray action probability density functions, which are both insightful and useful. Also, that approach gives a proper treatment of scattering near the sound channel axis. (The treatment above – Eq. (43), for example – does not properly treat near-axial scattering as it does not account for the fact that I is nonnegative, with $I = 0$ on the sound channel axis.)

Figure 3 shows a quantity closely related to $\omega'(I)$ for experimental conditions corresponding to the wavefields shown in Fig. 1. The quantity plotted in Fig. 3, $\alpha(I) = I\omega'(I)/\omega(I)$, is a nondimensional measure of $\omega'(I)$. (Under conditions appropriate for this figure, axial ray angle $\varphi(z_{axis})$ is a monotonically increasing function of action I. The relationship between ray angle $\varphi(z)$ and action I follows from $dz/dr = p = \sqrt{2[\mathcal{H}(I) - V(z)]} = \tan \varphi(z)$.) This figure shows that there are large variations in $\omega'(I)$ for shallow angle (less than about 5 degrees) rays, corresponding to late-arriving energy, while $|\omega'(I)|$ is small for the steep (between approximately 6 and 12 degrees) rays, corresponding to early-arriving energy [42]. This dependence is consistent with the aforementioned dependence of scattered wavefield

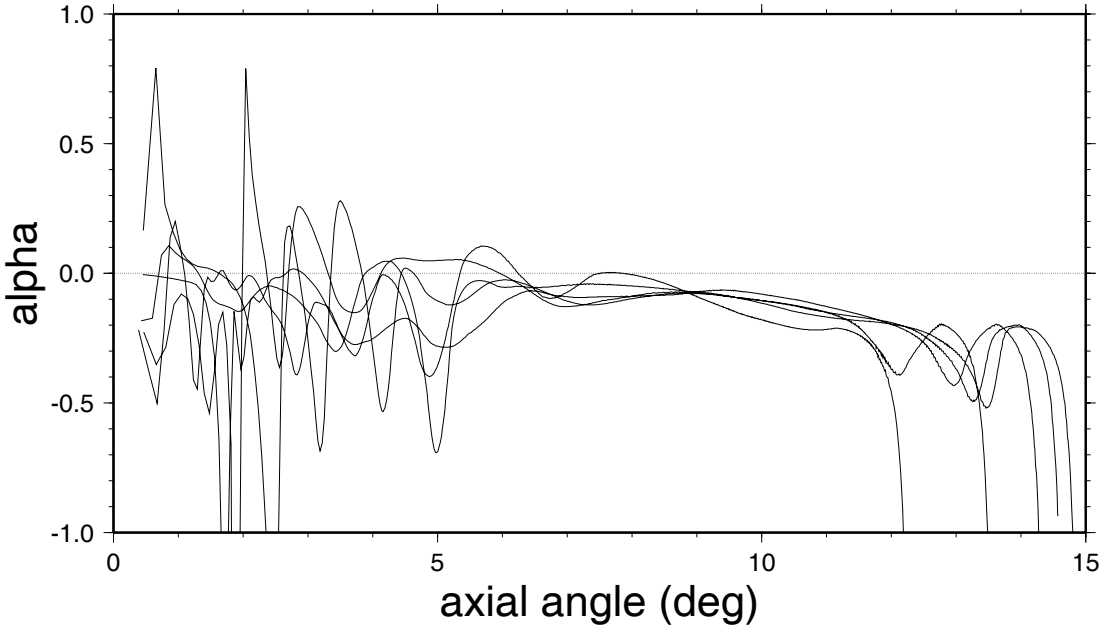

FIG. 3: Stability parameter α versus axial ray angle φ in the environment corresponding to the wavefields shown in Fig. 1. Each of the five $\alpha(\varphi(z_{axis}))$ curves was computed from a 650 km range-average of environmental measurements [18] along the 3250 km transmission path. Taken with permission from Ref. [8].

properties on $\omega'(I)$ and Fig. 1: the early steep ray arrivals (which encounter strong sound speed fluctuations) are relatively stable with small time spreads; the late flat ray arrivals (which encounter weak sound speed fluctuations) are less stable and have larger time spreads. These observations suggest strongly, albeit in a non-quantitative fashion, that properties of finite frequency wavefields are indeed controlled to a large extent by $\omega'(I)$.

V. DISCUSSION

Although we have adopted a tutorial tone in this review, it should be clear from the discussion that many fundamental issues remain unsolved. The first such set of issues relate to the usual problems associated with wave chaos. Realistic deep ocean environments have range- as well as depth-dependence, and in such environments ray trajectories exhibit extreme sensitivity associated with chaotic motion. In spite of this, finite frequency wavefields, both measured and simulated, show remarkable stability. The wave chaos challenge is to reconcile ray instability with wavefield stability. Surprisingly, wavefield stability can be partially explained using ray arguments: although individual rays are predominantly chaotic, continuous collections of rays (corresponding to a point source with a broad angular aperture, for instance) are surprisingly stable. This is linked to a phenomenon that has been referred to as 'manifold stability' [40]. Finite-frequency effects, of course, also serve to mitigate against extreme sensitivity [16], but this introduces a new level of difficulty and more questions. The relationship between ray amplitude statistics [25] and

wavefield intensity statistics [19] is not well understood; the proliferation of eigenray contributions and the necessity of applying caustic corrections to the ray amplitudes constitute significant complications.

In view of these difficulties one might ask whether one should bother at all with the ray description. There are at least two strong reasons to continue to use ray methods and to try to better understand the wave chaos enigma. First, the ray-like character of underwater acoustic wavefield measurements strongly suggests that the ray description is both useful and approximately valid. Second, the ray description is physically insightful, providing critically important insight into the underlying propagation physics that is difficult to obtain by any other means.

In this chapter we have focused on the class of problems for which $c(z,r) = c(z) + \delta c(z,r)$ as this assumption is applicable in a wide variety of underwater acoustic environments. Provided $\delta c(z,r)$ can be accurately approximated as a multiperiodic function of r, a fairly complete understanding of the ray dynamics follows in the form of a KAM theorem and associated theory. Also, for this class of problems a stochastic description of ray motion is approximately valid and has proven to be useful. Interestingly, however, the connection between the dynamical-systems-based results and the stochastic description is not well understood. For instance, because the mechanism leading to torus destruction and the loss of ray stability is the excitation and overlapping of low-order resonances, and because resonance widths are controlled by $|\omega'(I)|$, one expects that that ray diffusion in action (I) is controlled in part by $|\omega'(I)|$, but no such connection has been established. At least in the study of the class of problems on which we have focused, there is reason for optimism. Namely, the action-angle formalism ties together all of the subjects that we have discussed: integrable systems, modes and mode coupling, deterministic chaos and resonances, and stochastic approximations. Thus, it is reasonable to expect that an action-angle-based description will provide valuable insight into many of the questions that we have raised and tie together seemingly unrelated issues.

Acknowledgments

We thank Javier Beron-Vera, Nicholas Cerruti, Katherine Hegewisch, Irina Rypina, and Ilya Udovydchenkov for the benefit of many discussions relating to the material presented and to the editors for their help and patience. Also, we gratefully acknowledge support from the US National Science Foundation, grants PHY-0555301 (ST) and CMG-0417425 (MB), and Code 321 of the Office of Naval Research (MB).

[1] S. M. Flatté, R. Dashen, W. H. Munk, and F. Zachariasen, *Sound Transmission through a Fluctuating Ocean* (Cambridge University Press, Cambridge, 1979).
[2] W. H. Munk, P. Worcester, and C. Wuncsh, *Ocean Acoustic Tomography* (Cambridge University Press, Cambridge, 1995).
[3] D. R. Palmer, M. G. Brown, F. D. Tappert, and H. F. Bezdek, Geophys. Res. Lett. **15**, 569 (1988).
[4] D. R. Palmer, T. M. Georges, and R. M. Jones, Comput. Phys. Commun. **65**, 219 (1991).
[5] K. B. Smith, M. G. Brown, and F. D. Tappert, J. Acoust. Soc. Am. **91**, 1939 (1992).
[6] K. B. Smith, M. G. Brown, and F. D. Tappert, J. Acoust. Soc. Am. **91**, 1950 (1992).
[7] M. G. Brown, J. A. Colosi, S. Tomsovic, A. L. Virovlyansky, M. A. Wolfson, and G. M. Zaslavsky, J. Acoust. Soc. Am. **113**, 2533 (2003), nlin.CD/0109027.
[8] F. J. Beron-Vera, M. G. Brown, J. A. Colosi, S. Tomsovic, A. L. Virovlyansky, M. A. Wolfson, and G. M. Zaslavsky, J. Acoust. Soc. Am. **114**, 1226 (2003), nlin.CD/0301026.
[9] M. L. Mehta, *Random Matrices (Third Edition)* (Elsevier, Amsterdam, 2004).
[10] T. A. Brody, J. Flores, J. B. French, P. A. Mello, A. Pandey, and S. S. M. Wong, Rev. Mod. Phys. **53**, 385 (1981).
[11] K. B. Efetov, *Supersymmetry in Disorder and Chaos* (Cambridge University Press, Cambridge, 1999).
[12] A. D. Mirlin, Phys. Rep. **326**, 259 (2000).
[13] M. C. Gutzwiller, *Chaos in Classical and Quantum Mechanics* (Springer-Verlag, New York, 1990).
[14] M. J. Giannoni, A. Voros, and J. Jinn-Justin, eds., *Chaos and Quantum Physics* (North-Holland, Amsterdam, 1991).
[15] M. Brack and R. K. Bhaduri, *Semiclassical Physics* (Westview Press, Boulder, 2003).
[16] K. C. Hegewisch, N. R. Cerruti, and S. Tomsovic, J. Acoust. Soc. Am. **117**, 1582 (2001).
[17] W. H. Munk, in *Evolution of Physical Oceanography*, edited by B. A. Warren and C. Wunsch (MIT Press, Cambridge, 1981), pp. 264–291.
[18] P. F. Worcester, B. D. Cornuelle, M. A. Dzieciuch, W. H. Munk, B. M. Howe, J. A.Mercer, R. C. Spindel, J. A. Colosi, K. Metzger, T. Birdsall, et al., J. Acoust. Soc. Am. **105**, 3185 (1999).
[19] J. A. Colosi, E. K. Scheer, S. M. Flatté, B. D. Cornuelle, M. A. Dzieciuch, W. H. Munk, P. F. Worcester, B. M. Howe, J. A.Mercer, R. C. Spindel, et al., J. Acoust. Soc. Am. **105**, 3202 (1999).
[20] F. D. Tappert, in *Lecture Notes in Physics, Vol.* **70***, Wave propagation and underwater acoustics*, edited by J. B. Keller and J. S. Papadakis (Springer-Verlag, New York, 1977), pp. 224–287.
[21] H. Goldstein, *Classical mechanics* (Addison-Wesley, Reading, 1980).
[22] M. Tabor, *Chaos and Integrability in Nonlinear Dynamics: An Introduction* (Wiley, New York, 1989), see pp. 20-31.

[23] A. L. Virovlyansky, A. Y. Kazarova, and L. Y. Lyubavin, Wave Motion **42**, 317 (2005).
[24] V. I. Arnol'd, *Mathematical Methods of Classical Mechanics* (Springer, Berlin, 1978).
[25] M. A. Wolfson and S. Tomsovic, J. Acoust. Soc. Am. **109**, 2693 (2001).
[26] P. Grassberger, R. Badii, and A. Politi, J. Stat. Phys. **51**, 135 (1988).
[27] E. Ott, *Chaos in Dynamical Systems* (Cambridge University Press, Cambridge, 2002).
[28] B. V. Chirikov, Phys. Rep. **52**, 263 (1979).
[29] J. A. Colosi and M. G. Brown, J. Acoust. Soc. Am. **103**, 2232 (1998).
[30] A. Jorba and C. Simo, SIAM J. Math. Anal. **27**, 1704 (1996).
[31] M. B. Sevryuk, Dis. Cont. Dyn. Sys. **18**, 569 (2007).
[32] I. I. Rypina, M. G. Brown, F. J. Beron-Vera, H. Koak, M. J. Olascoaga, and I. A. Udovydchenkov, Phys. Rev. Lett. **98**, 104102 (2007).
[33] B. V. Chirikov, At. Energ. **6**, 630 (1959), russian; English J. Nucl. Energy Part C: Plasma Phys. **1**, 253 (1960).
[34] F. J. Beron-Vera and M. G. Brown, J. Acoust. Soc. Am. **114**, 122 (2003).
[35] F. J. Beron-Vera and M. G. Brown, J. Acoust. Soc. Am. **115**, 1068 (2004).
[36] F. J. Beron-Vera and M. G. Brown, J. Acoust. Soc. Am. (2008), submitted.
[37] I. I. Rypina and M. G. Brown, J. Acoust. Soc. Am. **122**, 1440 (2007).
[38] I. A. Udovydchenkov and M. G. Brown, J. Acoust. Soc. Am. **123**, 41 (2008).
[39] A. L. Virovlyansky, A. Y. Kazarova, and L. Y. Lyubavin, J. Acoust. Soc. Am. **121**, 2542 (2007).
[40] N. R. Cerruti and S. Tomsovic, Phys. Rev. Lett. **88**, 054103 (2002).
[41] We have adapted the term quantization from quantum mechanics, but in this context, action quantization refers to the determination of the *discrete* set of rays and their classical actions which directly correspond to the modes.
[42] The fact that shallow rays arrive later than steep rays may be counterintuitive because the shallow rays travel a shorter distance, however in the ocean's sound channel the path length decrease turns out to be more than offset by the slower mean velocity.